3714 *Inorg. Chem.* **1998,** *37,* 3714−3718

Proton NMR Study of Oxo-Bridged Dimanganese(III) Complexes: Solution State Structures and an Isotropic Shift/Magnetic Exchange Correlation

David W. Wright,[†] Henry J. Mok, Christopher E. Dubé, and William H. Armstrong*

Department of Chemistry, Eugene F. Merkert Chemistry Center, Boston College,
Chestnut Hill, Massachusetts 02167-3860

Received May 30, 1996

The ^{1}H NMR spectra of a series of manganese−oxo aggregates have been examined, and a characteristic signature was found for each complex. For the dimanganese(III,III) complexes $[\mathrm{Mn_2O(OAc)_2(HB(pz)_3)_2}]$, $[\mathrm{Mn_2O(OAc)_2(tacn)_2}]^{2+}$, $[\mathrm{Mn_2O(OAc)_2(H_2O)_2(bpy)_2}]^{2+}$, and $[\mathrm{Mn_2O(OAc)_2(bpta)_2}]^{2+}$ (HB(pz)$_3$ = hydrotris(pyrazol-1-yl)borate; tacn = 1,4,7-triazacyclononane; bpy = 2,2′-bipyridine, and bpta = *N*,*N*-bis(2-pyridylmethyl)-*tert*-butylamine), the ^{1}H NMR spectra reveal a resonance associated with acetate, found downfield between 58 and 80 ppm, and a generally well resolved set of terminal ligand resonances which can be divided into two classes: those resonances associated with pyridyl or pyrazolyl ring protons and those of methylene groups. A number of the pyridine ring resonances have been unambiguously assigned by the examination of methyl-substituted derivatives. Data for these derivatives also support a coordination geometry-dependent pathway for spin delocalization. Moreover, interpretation of the ^{1}H NMR spectra leads to the conclusion that the solution-state structures of all members of the series are the same as the reported solid-state structures. A strong linear correlation between the magnetic coupling constant (J) and the isotropic shift of the acetate resonance was observed within this series of $\{\mathrm{Mn_2O(OAc)_2}\}^{2+}$ core complexes. Furthermore, comparisons of the acetate proton isotropic shift ratio ($\Delta H_{\mathrm{Mn}}/\Delta H_{\mathrm{Fe}}$) to the ratio of the squared effective magnetic moments $\mu_{\mathrm{eff}}{}^2(\mathrm{Mn})/\ \mu_{\mathrm{eff}}{}^2(\mathrm{Fe})$ for complexes with the $\{\mathrm{M_2O(OAc)_2}\}^{2+}$ core (where M = Mn^{3+} or Fe^{3+}) revealed excellent agreement (within 10%) between these two quantities.

Introduction

Polynuclear manganese aggregates are found at the active sites of a variety of metalloenzymes. Among the enzymes believed to have dinuclear Mn centers are certain bacterial thiosulfate oxidases,[1] catalases,[2] and ribonucleotide reductases.[3] Based on spectroscopic evidence as well as the low-resolution crystal structure of the Mn-containing catalase from *Thermus thermophilus*, the manganese centers of these enzymes have been formulated as a $\{\mathrm{Mn_2}(\mu\text{-OH})(\mu\text{-O_2CR})_2\}$ or $\{\mathrm{Mn_2}(\mu\text{-O})(\mu\text{-O_2CR})_2\}$ core with peripheral histidine imidazole ligands.[4] In part because of the lack of high-resolution structural data for the manganese centers in these enzymes, a number of investigators have undertaken the synthesis and structural characterization of low-molecular-weight complexes in order to accurately model the physical properties of these metalloproteins.[5]

While the growing number of synthetic approaches to higher valent multinuclear manganese−oxo clusters[5−12] and the wide array of ligands which can be used to help control aggregation have produced a variety of intriguing complexes, the characterization of the vast majority of these complexes has relied predominantly on X-ray crystallographic solid-state structures, complimented by EPR, electrochemistry, and magnetic suscep-

---

[†] Present address: Duquesne University, Department of Chemistry and Biochemistry, Pittsburgh, PA 15282.

(1) Cammack, R.; Chapman, A.; Lu, W.-P.; Karagouni, A.; Kelly, D. P. *FEBS Lett.* **1989**, *253*, 239.

(2) (a) Jones, D.; Diebel, D. H.; Niven, C. F., Jr. *J. Bacteriol.* **1965**, *88*, 602. (b) Kono, Y.; Fridovich, I. *J. Biol. Chem.* **1983**, *258*, 6015. (c) Algood, G. S.; Perry, J. *J. Bacteriol.* **1986**, *168*, 563. (d) Barynim, V. V.; Grebenko, A. *Dokl. Akad. Nauk SSSR* **1986**, *228*, 877.

(3) (a) Schimpff-Weiland, G.; Follman, H.; Auling, G. *Biochem. Biophys. Res. Commun.* **1981**, *102*, 1276. (b) Willing, A.; Follman, H.; Auling, G. *Eur. J. Biochem.* **1988**, *170*, 603.

(4) (a) Barynin, V. V.; Vagin, A. A.; Melik-Adamyan, V. R.; Grebenko, A. I.; Khangulov, S. V.; Popov, A. N.; Andrianova, M. E.; Vainstein, B. K. *Dokl. Akad. Nauk SSSR* **1986**, *228*, 877. (b) Waldo, G. S.; Yu, S.; Penner-Hahn, J. E. *J. Am. Chem. Soc.* **1992**, *114*, 5869. (c) Waldo, G. S.; Penner-Hahn, J. E. *J. Am. Chem. Soc.* **1995**, *117*, 1507. (d) Khangulov, S. V.; Pessiki, P. J.; Barynin, V. V.; Ash, D. E.; Dismukes, G. C. *Biochemistry* **1995**, *34*, 2015.

(5) (a) Armstrong, W. H. In *Manganese Redox Enzymes*; Pecoraro, V. L. Ed.; VCH: New York, 1992; p 261. (b) Brudvig, G. W.; Thorp, H. H.; Crabtree, R. H. *Acc. Chem. Res.* **1991**, *24*, 311. (c) Manchanda, R.; Brudvig, G. W.; Crabtree, R. H. *Coord. Chem. Rev.* **1995**, *144*, 1. (d) Dave, B. C.; Czernuszewicz, R. S. *New J. Chem.* **1994**, *18*, 149. (e) Thorp, H. H.; Brudvig, G. W. *New J. Chem.* **1991**, *15*, 479.

(6) (a) Cooper, S. R.; Calvin, M. *J. Am. Chem. Soc.* **1977**, *99*, 6623. (b) Stebler, M.; Ludi, A.; Bürgi, H.-B. *Inorg. Chem.* **1986**, *25*, 4743.

(7) (a) Mandal, S. K.; Armstrong, W. H. *Inorg. Chim. Acta* **1995**, *229*, 261. (b) Mok, H. J.; Davis, J. A.; Pal, S.; Mandal, S. K.; Armstrong, W. H. *Inorg. Chim. Acta* **1997**, *263*, 385. (c) Pal, S.; Chan, M. K.; Armstrong, W. H. *J. Am. Chem. Soc.* **1992**, *114*, 6398.

(8) (a) Vincent, J. B.; Christmas, C.; Chang, H.-R.; Li, Q.; Boyd, P. D. W.; Huffman, J. C.; Hendrickson, D. N.; Christou, G. *J. Am. Chem. Soc.* **1989**, *111*, 2086. (b) Libby, E.; McGisker, J. K.; Schmitt, E. A.; Folting, K.; Hendrickson, D. N.; Christou, G. *Inorg. Chem.* **1991**, *30*, 3486.

(9) (a) Hendrickson, D. N.; Christou, G.; Schmitt, E. A.; Libby, E.; Bashkin, J. S.; Wang, S.; Tsai, H.-L.; Vincent, J. B.; Boyd, P. D. W.; Huffman, J. C.; Folting, K.; Li, Q.; Streib, W. E. *J. Am. Chem. Soc.* **1992**, *114*, 2455. (b) Wemple, M. W.; Tsai, H.-L.; Folting, K.; Hendrickson, D. N.; Christou, G. *Inorg. Chem.* **1993**, *32*, 2025. (c) Wemple, M. W.; Adams, D. M.; Folting, K.; Hendrickson, D. N.; Christou, G. *J. Am. Chem. Soc.* **1995**, *117*, 7275.

(10) (a) Menage, S.; Girerd, J.-J.; Gleizes, A. *J. Chem. Soc., Chem. Commun.* **1988**, 431. (b) Vincent, J. B.; Tsai, H.-L.; Blackman, A. G.; Wang, S.; Boyd, P. D. W.; Folting, K.; Huffman, J. C.; Lobkovsky, E. B.; Hendrickson, D. N.; Christou, G. *J. Am. Chem. Soc.* **1993**, *115*, 12353.

(11) Vincent, J. B.; Chang, H.-R.; Folting, K.; Huffman, J. C.; Christou, G.; Hendrickson, D. N. *J. Am. Chem. Soc.* **1987**, *109*, 5703.

(12) (a) Matsushita, T.; Spenser, L.; Sawyer, D. T. *Inorg. Chem.* **1988**, *27*, 1167. (b) Gohdes, J. W. Doctoral Thesis, University of California, Berkeley, 1992.

S0020-1669(96)00646-5 CCC: $15.00

tibility studies. Although manganese(III) is a potentially favorable paramagnetic transition metal ion for observing ligand proton resonances,[20] ^{1}H NMR spectra have been reported for few manganese(III) complexes.[8,13,14,29] Herein, the ^{1}H NMR "fingerprint" of the ligated $\{Mn_2O(OAc)_2\}^{2+}$ core is reported. The spectra suggest that the complexes maintain their solid-state structures in solution. Additionally, ^{1}H isotropic shifts provide insight into the operative spin delocalization mechanisms for these complexes and can be correlated with bulk magnetic properties, further corroborating that the solution-state and solid-state structures are very similar.

Experimental Methods

Abbreviations. The following abbreviations are used throughout this paper: OAc, acetate; bpy, 2,2′-bipyridine; 4,4′-dmb, 4,4′-dimethyl-2,2′-bipyridine; tacn, 1,4,7-triazacyclononane; Me_3tacn, 1,4,7-trimethyl-1,4,7-triazacyclononane; $HB(pz)_3^-$, hydrotris(pyrazol-1-yl)borate; bpma, *N*,*N*-bis(2-pyridylmethyl)methylamine; bpea, *N*,*N*-bis(2-pyridylmethyl)ethylamine; bpta, *N*,*N*-bis(2-pyridylmethyl)-*tert*-butylamine; *X*,*X*′-Me_2bpxa, 4,4′(5,5′)-dimethyl-*N*,*N*-bis(2-pyridylmethyl)-X-(X = methyl, ethyl, or *tert*-butyl)amine.

General. All reagents and solvents were purchased from commercial sources and used as received, unless noted otherwise. Acetonitrile and diethyl ether were distilled under nitrogen from CaH_2 and sodium/benzophenone, respectively, prior to use. $[Mn_2O(OAc)_2(HB(pz)_3)_2]$ (**1**),[13] $[Mn_2O(OAc)_2(tacn)_2](ClO_4)_2$ (**2**),[15] $[Mn_2O(OAc)_2(Me_3tacn)_2](ClO_4)_2$ (**3**),[15] $[Mn_2O(OAc)_2(H_2O)_2(bpy)_2](BF_4)_2$ (**4**),[10a] $[Mn_2O(OAc)_2(bpy)_2(Cl)_2]$ (**5**),[10b] and $[Mn_2O(OAc)_2(bpta)_2](ClO_4)_2$ (**6**)[7b] were synthesized according to literature procedures. (For ligand structures, numbering schemes, and abbreviations, see Figure 1.) The identity and purity of these complexes were confirmed by UV−vis spectroscopy and elemental analysis (see Supporting Information). Elemental analysis was performed by Robertson Analytical Laboratories, Madison, NJ. The deuterated acetate analogues (denoted as **-d$_3$**) of the $Mn_2^{III,III}$ dinuclear complexes were synthesized according to literature methods as cited above. All samples were examined by EPR to ensure the absence of Mn^{II} and dinuclear $Mn_2^{III,IV}$ contaminants.

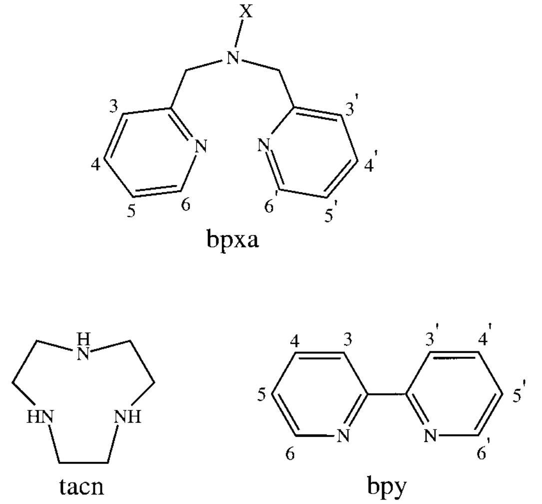

Figure 1. Ligand structures, numbering schemes, and abbreviated names used in this text.

Ligand Synthesis. ***N*,*N*-Bis(2-pyridylmethyl)-X-amine (bpxa, where X = m (methyl), e (ethyl), or t (*tert*-butyl)).** Synthesis of the bpxa ligand series (see Supporting Information) was modified from the previously reported synthesis of bpea by Pal et al.[7c] The bpta ligand used here was synthesized as reported elsewhere.[7b]

5(4)-Methyl-2-picolyl Chloride Hydrochloride. Synthesis of the methyl-substituted picolyl chloride hydrochloride was based on procedures described by K. D. Karlin (personal communication).[30] The 5-methyl- and 4-methyl-substituted picolyl chloride hydrochloride were prepared by using the same method. A solution of 16.5 g (0.154 mol) of 2,5(2,4)-lutidine, 90 mL of glacial acetic acid, and 28 mL of 30% (by w/w) hydrogen peroxide was heated to reflux for 12 h. The crude product, 2,5(2,4)-lutidine-*N*-oxide, was dried by rotary evaporation, redissolved in $CHCl_3$, and dried over anhydrous K_2CO_3 for several hours. The $CHCl_3$ mixture was filtered through Celite and subsequently concentrated by rotary evaporation to an oil. The *N*-oxide oil was dried over NaOH pellets for several hours, filtered, and added to 30 mL of boiling acetic anhydride. This solution was refluxed for 6 h. The mixture was cooled to room temperature, diluted with methanol, and evaporated to dryness. The 2-(acetoxymethyl)-4-methylpyridine was purified by distillation. The high purity of 2-(acetoxymethyl)-5-methylpyridine, as shown by ^{1}H NMR, made distillation unnecessary. The 2-(acetoxymethyl)-5(4)-methylpyridine was heated to reflux in 100 mL of 2 N NaOH for 18 h. When cooled, the solution was extracted with diethyl ether, and the ether extracts were dried by rotary

---

(13) Sheats, J. E.; Czernuszewicz, R. S.; Dismukes, G. C.; Rheingold, A. L.; Petrouleas, V.; Stubbe, J.; Armstrong, W. H.; Beer, R.; Lippard, S. J. *J. Am. Chem. Soc.* **1987**, *109*, 1435.

(14) Bonadies, J. A.; Maroney, M. J.; Pecoraro, V. L. *Inorg. Chem.* **1989**, *28*, 2044.

(15) Wieghardt, K.; Bossek, U.; Ventur, D.; Weiss, J. *J. Chem. Soc., Chem. Commun*. **1985**, 347.

(16) *VNMRS Software*, Revision 4.1C; Varian Nuclear Magnetic Resonance Instruments: Palo Alto, CA, 1989−1992.

(17) Swift, T. J. In *NMR of Paramagnetic Molecules*; La Mar, G. N., Horrocks, H. deW., Jr., Holm, R. H., Eds.; Academic Press: New York, 1973; p 53.

(18) Lachicotte, R.; Kitaygorodskiy, A.; Hagen, K. S. *J. Am. Chem. Soc.* **1993**, *115*, 8883.

(19) (a) Schlager, O.; Wieghardt, K.; Grondey, H.; Rufinska, A.; Nuber, B. *Inorg. Chem.* **1995**, *34*, 6440. (b) Schlager, O.; Wieghardt, K.; Nuber, B. *Inorg. Chem.* **1995**, *34*, 6456.

(20) Horrocks, H. deW., Jr. In *NMR of Paramagnetic Molecules*; La Mar, G. N., Horrocks, H. deW., Jr., Holm, R. H., Eds.; Academic Press: New York, 1973; p 159.

(21) Bertini, I.; Luchinat, C. In *Physical Methods for Chemists*; Drago, R. S., Ed.; Harcourt Brace Javonovich: Ft. Worth, TX, 1992; p 500.

(22) For all of the complexes examined herein, no cross-peaks were observed for NOESY, COSY, or TOCSY 2D NMR methods. Experimental parameters were those established in the following reference for the structurally related $\{Fe_2O(OAc)_2\}$ core and modified as appropriate for the manganese complexes: Li-June, M.; Jang, H. G.; Que, L., Jr. *Inorg. Chem.* **1992**, *31*, 359.

(23) Le Mar, G. N.; Eaton, G. R.; Holm, R. H.; Walker, F. A. *J. Am. Chem. Soc.* **1973**, *95*, 63.

(24) (a) Shteinman, A. A. *Mendeleev Commun.* **1992**, 155. The reported value of μ_{eff} determined by the Evan's method produced a range of values between 1.6 and 1.7. When resonable error estimates are included, the level of imprecision is evident. (b) Vincent, J. B.; Huffman, J. C.; Christou, G.; Li, Q.; Nanny, M. A.; Hendrickson, D. N.; Fong, R. H.; Fish, R. H. *J. Am. Chem. Soc.* **1988**, *110*, 6898.

(25) Que, L., Jr.; True, A. E. In *Progress in Inorganic Chemistry*; Lippard, S. J., Ed.; John Wiley-Interscience: New York, 1990; Vol. 38, p 109.

(26) Gorun, S. M.; Lippard, S. J. *Inorg. Chem.* **1991**, *30*, 1625.

(27) Surprisingly, the tacn complexes are in good agreement with theory, in spite of the unexpectedly low coupling constant of $J = -84$ cm^{-1} for the Fe complex previously noted by several authors (refs 25, 26). In particular, the reported value does not follow the previously reported empirical magnetostructural correlation reported by Gorun and Lippard for over 36 coupled $\{Fe_2O\}^{4+}$ centers. A reexamination of the magnetic properties of this compound resulted in a J value of -120 cm^{-1}.

(28) Satcher, J. H.; Balch, A. L. *Inorg. Chem.* **1995**, *34*, 3371.

(29) Hage, R.; Gunnewegh, E. A.; Niül, J.; Tjan, F. S. B.; Weyhermüller, T.; Wieghardt, K. *Inorg. Chim. Acta* **1998**, *268*, 43.

(30) (a) Hardegger, E.; Nikles, E. *Helv. Chim. Acta* **1957**, *40*, 2428. (b) Yoshio, A.; Achiwa, K. *Yakugaku Zasshi* **1959**, *79*, 108. (c) Baker, W.; Buggle, K. M.; McOmie, J. F. W.; Watkins, D. A. M. *J. Chem. Soc. (London)* **1958**, 3594.

(31) (a) Armstrong, W. H.; Spool, A.; Papaefthymiou, G. C.; Frankel, R. B.; Lippard, S. J. *J. Am. Chem. Soc.* **1984**, *106*, 3653. (b) Hartman, J. R.; Rardin, R. L.; Chaudhuri, P.; Pohl, K.; Wieghardt, K.; Nuber, B.; Weiss, J.; Papaefthymiou, G. C.; Frankel, R. B.; Lipard, S. L. *J. Am. Chem. Soc.* **1987**, *109*, 7387. (c) Wieghardt, K.; Pohl, K.; Gerbert, W. *Angew. Chem., Int. Ed. Engl.* **1983**, *22*, 727. (d) Arafa, I. M.; Goff, H. M.; David, S. S.; Murch, B. P.; Que, L., Jr. *Inorg. Chem.* **1987**, *26*, 2779.

(32) Que, L., Jr.; Maroney, M. J. In *Metal Ions in Biological Systems*; Sigel, H., Ed.; Marcel Decker, Inc.: New York, 1987; Vol. 21, p 87.

evaporation. For every 1.6 g of the crude 2-(hydroxymethyl)-5(4)-methylpyridine, cooled to 0 °C, 30 mL of neat thionyl chloride was added dropwise. The mixture was warmed to 50 °C for 6 h and immediately thereafter evaporated to dryness. Solid 5(4)-methyl-2-picolyl chloride hydrochloride was obtained in a yield of 54.4% (12.6%). The isolated 14.92 (3.45) g of 5(4)-methyl-2-picolyl chloride hydrochloride was of sufficient purity for use in the syntheses of the 5,5′(4,4′)-dimethyl-substituted bpxa ligands. 300-MHz ^{1}H NMR in $CDCl_3$ referenced to residual $CHCl_3$: for 5-methyl-2-picolyl chloride hydrochloride, 2.58 (s) 5-CH_3, 5.16 (s) 2-CH_2Cl, 7.96 (d) 3-H, 8.23 (d) 4-H, 8.55 (s) 6-H; for 4-methyl-2-picolyl chloride hydrochloride, 2.69 (s) 4-CH_3, 5.16 (s) 2-CH_2Cl, 7.67 (d) 5-H, 7.84 (s) 3-H, 8.57 (d) 6-H.

N,N-Bis(5(4)-methyl-2-pyridylmethyl)-X-amine (5,5′(4,4′)-Me$_2$bpxa, where X = m (methyl), e (ethyl), or t (*tert*-butyl)). Preparations of all methyl-substituted ligands series were analogous to those of their unsubstituted counterparts (see Supporting Information).[7b,c] 300-MHz ^{1}H NMR in $CDCl_3$ referenced to residual $CHCl_3$: for 5,5′-Me$_2$bpta, 1.26 (s) *tert*-butyl CH_3, 2.25 (s) 5,5′-CH_3, 4.65 (s) methylene, 7.38 (d) 3,3′-pyridyl H's, 7.54 (d) 4,4′-pyridyl H's, 8.41 (s) 6,6′-pyridyl H's; for 4,4′-Me$_2$bpta: 1.17 (s) *tert*-butyl CH_3, 2.22 (s) 4,4′-CH_3, 3.89 (s) methylene, 6.79 (d) 5,5′-pyridyl H's, 7.24 (s) 3,3′-pyridyl H's, 8.22 (d) 6,6′-pyridyl H's. Yields in accord with ^{1}H NMR and GC/MS data: 5,5′-Me$_2$bpta, 34%; 4,4′-Me$_2$bpta, 12%.

Synthesis of Methyl-Substituted Analogues. [$Mn_2O(OAc)_2$(4,4′-Me$_2$bpta)$_2$](ClO_4)$_2$ (7), [$Mn_2O(OAc)_2$(5,5′-Me$_2$bpta)$_2$](ClO_4)$_2$ (8), and [$Mn_2O(OAc)_2Cl_2$(4,4′-dmb)$_2$] (9). The preparations of the methyl-substituted analogues of [$Mn_2O(OAc)_2(bpta)_2$](ClO_4)$_2$ (**6**)[7b] and [$Mn_2O(OAc)_2(bpy)_2Cl_2$] (**5**)[10b] were based on literature methods (see Supporting Information).

The yield of **7** was 414 mg (43.4%). For the synthesis of **8**, the reaction scale was increased 3-fold to yield 1.32 g (40.9%). Complex **9** is more soluble in MeCN than the parent compound, forming small red-brown crystals after several days of concentration under ambient conditions. The crystals were collected by filtration, washed with MeCN and Et_2O, and dried in air. The yield of **9** was 37%.

Physical Measurements. ^{1}H NMR spectra were recorded at ambient temperature (probe temperature 294−295 K) on a Varian Unity 300 spectrometer. Samples that were nearly saturated in manganese complex (3−5 mM) required 256−1000 acquisitions to obtain satisfactory signal-to-noise ratios. Data collection parameters for the standard proton pulse sequence include a spectral width of 100 kHz, with 64 000 time domain points. All ^{1}H NMR spectra were baseline corrected using a simple first-order correction function. Values for chemical shifts (ppm) are the *observed* shifts referenced to residual solvent resonances. Residual protic solvent peaks were referenced as CHD_2CN, 1.95 ppm; CHD_2OD, 3.50 ppm; $CHCl_3$, 7.26 ppm; and $CHDCl_2$, 5.32 ppm.

EPR spectra were obtained at X-band with a Bruker ECS 106 spectrometer near 77 K using an immersion finger dewar filled with liquid nitrogen. Visible spectra were obtained in a convenient solvent using either a Perkin-Elmer 1-E or a Varian Lambda-3B spectrophotometer.

Results and Discussion

The proton spectra of [$Mn_2O(OAc)_2(tacn)_2$]$^{2+}$ (**2**), [$Mn_2O(OAc)_2(bpy)_2$]$^{2+}$ (**4**), and [$Mn_2O(OAc)_2(bpta)_2$]$^{2+}$ (**6**), shown in Figure 2, reveal a definitive fingerprint for the ligated {$Mn_2O(OAc)_2$}$^{2+}$ core, consisting of a characteristic acetate resonance and a distinctive pattern of terminal ligand resonances. The resonances associated with the bridging acetate groups, definitively assigned by synthesis of the deuterated acetate analogues, are found downfield between 58 and 80 ppm. Further, the ligand proton resonances can be divided into two classes, with the methylene resonances spanning a range of $+91 > \delta > -90$ ppm, while the pyridyl ring protons fall in the range $+53 > \delta > -90$ ppm (see Figure 2). The integrated intensities for the resonances of the acetate methyl groups and the ring protons are in good agreement with the predicted ratios from empirical formulas (see Supporting Information).

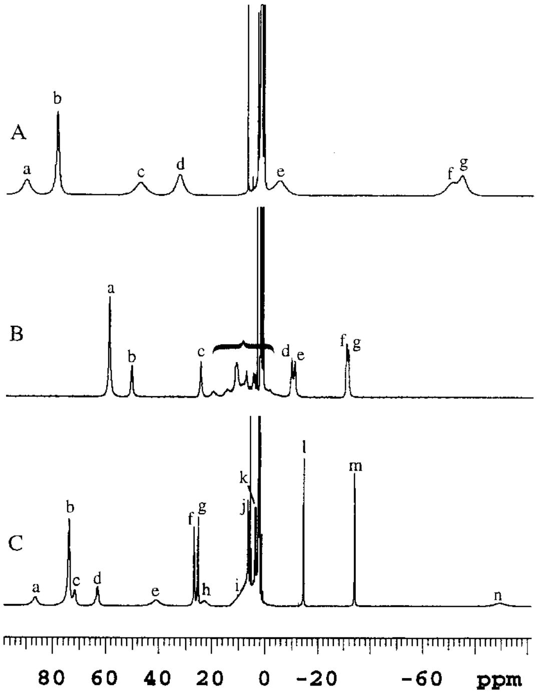

Figure 2. 300-MHz ^{1}H NMR spectra of complexes with the {$Mn_2(\mu\text{-}O)(\mu\text{-}OAc)_2$}$^{2+}$ core type in acetonitrile-d_3. (A) [$Mn_2O(OAc)_2(tacn)_2$](ClO_4)$_2$ (**2**); (B) [$Mn_2O(OAc)_2(H_2O)_2(bpy)_2$]($BF_4$)$_2$ (**4**); (C) [$Mn_2O(OAc)_2(bpta)_2$](ClO_4)$_2$ (**6**). Symbol: {, [$Mn_2O_2(bpy)_4$]$^{3+}$ contaminant (see Experimental Section for details).

In the ^{1}H NMR spectrum of [$Mn_2O(OAc)_2(tacn)_2$]$^{2+}$ (**2**, Figure 2A), the protons from the bridging acetate (peak b) are observed at 79.0 ppm, similar to the reported 78.0 ppm for the [$Mn_2O(OAc)_2(Me_3tacn)_2$](ClO_4)$_2$ (**3**),[29] and six resonances associated with the tacn ligand are detected (peaks a, c−g). Assuming idealized C_{2v} symmetry for complex **2**, three inequivalent methylene groups of the tacn ligand are expected, with each methylene group having two types of protons. One proton is in an axial position (H_{ax}), such that it is canted toward the Mn^{III} ion. The other proton is in an equatorial position (H_{eq}), thus directed away from the metal (see Supporting Information). An analysis of the resonance peak widths ($\nu_{1/2}$) for **2** reveals two sets of peaks, one with $\nu_{1/2}$ of ∼900 Hz (peaks a, d, and g) and one with $\nu_{1/2}$ of ∼1400 Hz (peaks c, e, and f). We suggest that those resonances with a larger $\nu_{1/2}$ correspond to the axial protons, while the sharper resonances correspond to the equatorial ones.[8a] The assigned pattern of axial and equatorial methylene resonances in these complexes is reminiscent of those observed in the related Fe(II) and Co(II) hydroxy-bridged Me$_3$tacn dimeric analogues,[18] as well as a number of M(III) monomeric complexes (where M(III) = V, Cr, Mn, Fe, and Co) formed with the hexadentate ligand 1,4,7-tris(*o*-aminobenzyl)-1,4,7-triazacyclononane.[19]

The ^{1}H spectrum of [$Mn_2O(OAc)_2(bpy)_2(H_2O)_2$]$^{2+}$ (**4**, Figure 2B) shows the prototypical resonance pattern for a {$Mn_2O(OAc)_2$}$^{2+}$ core with terminally coordinated pyridyl moieties. Under idealized C_2 symmetry, one predicts one resonance attributable to the equivalent CH_3 groups of the bridging acetate ligands and eight resonances arising from the inequivalent terminal pyridyl protons. Of the nine predicted resonances, eight are observed, with the acetate resonance at 59.2 ppm and seven additional peaks attributable to ring protons spanning the range $51.1 > \delta > -31.1$ ppm. Resonances f and g (Figure 2B) are assigned as the 4,4′ protons of bpy, since they are not observed in [$Mn_2O(OAc)_2$(4,4′-dmb)$_2Cl_2$] (**9**) (see Supporting Information).

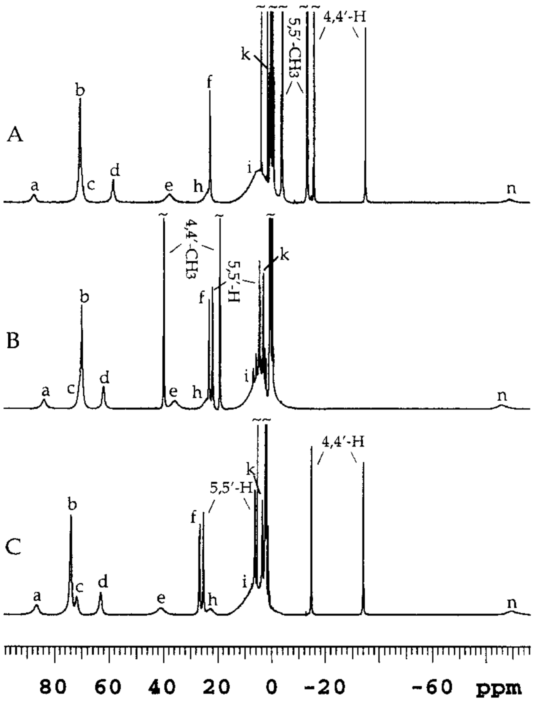

Figure 3. 300-MHz ^{1}H NMR spectra of complexes with the $\{Mn_2(\mu\text{-}O)(\mu\text{-}OAc)_2\}^{2+}$ core type in acetonitrile-d_3. (A) $[Mn_2O(OAc)_2(5,5'\text{-}Me_2bpta)_2](ClO_4)_2$ (**8**); (B) $[Mn_2O(OAc)_2(4,4'\text{-}Me_2bpta)_2](ClO_4)_2$ (**7**); (C) $[Mn_2O(OAc)_2(bpta)_2](ClO_4)_2$ (**6**). Symbol: ∼, truncated for scale.

Table 1. Proton NMR Data[a] for $[Mn_2O(OAc)_2(bpta)_2]^{2+}$ (**6**) and Related Complexes

6 (bpta)	**7** (4,4′-Me$_2$bpta)	**8** (5,5′-Me$_2$bpta)	assignment
86.5 (580)	85.1 (500)	89.0 (500)	$C^{meth}-H_{ax}$
73.9 (210)	71.4 (180)	72.0 (200)	O_2CCH_3
71.7 (400)	72.0 (420)		$C^{meth}-H_{eq}$
63.2 (290)	63.4 (270)	59.9 (270)	$C^{meth}-H_{eq}$
	41.2 (20)		4,4′-CH_3
41.0 (830)	37.2 (730)	39.3 (700)	$C^{meth}-H_{ax}$
26.7 (90)	24.7 (80)	24.5 (80)	3,3′-H
25.3 (80)	23.4 (70)		5,5′-H
22.7 (900)	25.6 (800)	25.5 (770)	6-H
	20.7 (20)		4,4′-CH_3
9.1		6.5 (2020)	N-$C(CH_3)_3$
6.4 (110)	6.1 (90)		5,5′-H
3.4 (110)	4.7 (90)	1.0	3,3′-H
		−2.2 (40)	5,5′-CH_3
		−11.5 (40)	5,5′-CH_3
−14.7 (50)		−14.1 (40)	4,4′-H
−34.1 (50)		−33.3 (40)	4,4′-H
−89.6 (1140)	−85.1 (850)	−87.0 (940)	6′-H

[a] Data are chemical shifts in ppm referenced to residual CD_2HCN (1.95 ppm) and, in parentheses, the full width at half-height ($\nu_{1/2}$) in hertz. See Experimental Section for additional details.

In the ^{1}H NMR spectrum of $[Mn_2O(OAc)_2(bpta)_2]^{2+}$ (**6**, Figure 2C), the acetate resonance appears at 73.9 ppm (peak b), while 12 additional resonances are observed spanning the range $87 > \delta > -90$ ppm. If an idealized C_2 symmetry, consistent with the reported crystal structure,[7b] is invoked for this complex, 14 resonances should be observed. The bpta ligand should contribute 13 resonances: four from each of the inequivalent pyridyl rings, four from each inequivalent proton of the two methylenes, and one from the nine equivalent protons from each of the *tert*-butyl groups. The six equivalent protons from the bridging acetate groups appear as a single resonance. Once solvent peaks are excluded, Figure 3A appears to show all 14 of the anticipated peaks. Table 1 provides the assignments for the ^{1}H spectrum of **6** based on resonance patterns obtained from the methyl-substituted analogues (Supporting Information). Combining $\nu_{1/2}$ analysis with comparisons to the spectrum of the tacn analogue (vide supra), the broad peaks are assigned as the methylene protons (peaks a, c, d, and e) and the 6,6′ protons of the pyridine rings (peaks h and n). The *tert*-butyl group protons of **6** are observed as a very broad peak (peak i) centered at 9.1 ppm that integrates to 18 protons (this broad peak is more clearly observed in the methyl-substituted complexes **7** and **8** included in Figure 2B and 2A). Based on the recently obtained crystal structure of **6**,[7b] the broadening of the *tert*-butyl group proton resonances can be attributed to hindered rotation around the N−$C(CH_3)_3$ bond of the ligand, which comes into close proximity to the bridging acetate groups of the core, producing short H···H distances in the van der Waals contact range.

The observed spectral patterns of the $\{Mn_2O(OAc)_2\}^{2+}$ dinuclear species arise from the disposition of ligands cis and trans with respect to the oxo bridge. For the high-spin Mn^{III} (d^4) case, if it is assumed that the d_{z^2} orbital of the Mn atom is oriented along the short Mn−oxide bond, then this orbital is presumed to become destabilized relative to the $d_{x^2-y^2}$ orbital and is, consequently, unoccupied. Thus, the pyridyl ring situated trans to the bridging oxide would be expected to be influenced predominately by a π-spin delocalization pathway from molecular d_π orbitals. In contrast, the pyridyl ring oriented cis to the bridging oxide ligand should be influenced by both σ- and π-spin delocalization pathways arising from the occupied metal $d_{x^2-y^2}$ and d_π orbitals, respectively. The alternating shift pattern observed for **6** around the ligand's pyridyl ring as well as the change in the sign of the isotropic shift between the H and Me resonances (Table 1) is clearly indicative of a dominating π-spin delocalization mechanism.[20,21] The attenuating influence of the σ-delocalization pathway is exemplified by the dramatic difference in the shifts of the 6′ and 6 protons (114 ppm) in $[Mn_2O(OAc)_2(bpta)_2]^{2+}$ (**6**). The 6′ proton of the pyridyl ligand trans to the oxide is contact shifted upfield by a π-spin delocalization pathway, while the 6 proton cis to the oxide is contact shifted downfield relative to the 6′ proton due to the influence of a σ-spin delocalization mechanism. In contrast, the difference between the resonance positions of the 4,4′ protons is 19.4 ppm, demonstrating the decreasing predominance of the σ-spin delocalization as it is propagated through the carbon bonds of the pyridyl moiety.

Although attempts to make definitive assignments of the core geometry using two-dimensional techniques proved unsuccessful,[22] the spectra demonstrate how the simple fingerprint of a core can be used to interpret more complex spectra. In this instance, the spectrum of $[Mn_2O(OAc)_2(tacn)_2]^{2+}$ shows the expected resonance pattern for the methylene moieties of the tacn ligand disposed around the core. Similarly, the spectrum of $[Mn_2O(OAc)_2(bpy)_2(H_2O)_2]^{2+}$ indicates the observed pattern for terminal pyridyl moieties. The spectrum for $[Mn_2O(OAc)_2(bpta)_2]^{2+}$, a complex whose ligand contains both methylene and pyridyl moieties, represents a composite of the above spectra, with many features mapping directly from the spectrum of **2** and **4**, respectively.

Magnetic Correlations. To a first approximation for isostructural iron and manganese complexes, the ratio of the isotropic shifts ($\Delta H_{Mn}/\Delta H_{Fe}$) will vary as the ratio of the molecular susceptibilities, χ_{Mn}/χ_{Fe}, or, equivalently, the ratio of the squared effective magnetic moments $\mu_{eff}^2(Mn)/\ \mu_{eff}^2(Fe)$ when the dipolar contributions to the chemical shift are negligible.[23] Previously, such an analysis has been applied successfully to the comparison of the chemical shift of the acetate resonance of $[Mn_2O(OAc)_2(HB(pz)_3)_2]$ (**1**) with its Fe

Table 2. Comparisons of the Square of the Ratio of the Effective Magnetic Moments, $\mu_{eff}^2(Mn)/\mu_{eff}^2(Fe)$, to the Ratio of the Isotropic Shifts ($\Delta H_{Mn}/\Delta H_{Fe}$) for Complexes with $\{Mn_2O(OAc)_2\}^{2+}$ and $\{Fe_2O(OAc)_2\}^{2+}$ Cores

	$\{Mn_2O(OAc)_2\}^{2+}$		$\{Fe_2O(OAc)_2\}^{2+}$				
ligand	μ_{eff}^2	ΔH_{iso}	μ_{eff}^2	ΔH_{iso}	$\mu_{eff}^2(Mn)/\mu_{eff}^2(Fe)$	$\Delta H_{Mn}/\Delta H_{Fe}$	difference (%)
$HB(pz)_3$	4.92[a]	63.5[a]	1.71[f]	8.4[f]	8.27	7.56	8.5
Me_3tacn	5.28[b]	80.4[c]	1.73[g]	8.9[h]	6.96	7.31	−5.0
tacn	5.12[b]	76.9[c]	1.84[i]	9.4[h]	7.74	8.18	−5.7
bpy/H_2O	3.86[d]	57.1[c]	1.6[j]	8.4[j]	5.82	6.79	−16.7
bpy/Cl	4.48[e]	58.5[c]	1.75[k]	8.6[c]	6.55	6.80	−3.8

[a] Reference 13. [b] Reference 15. [c] This work. [d] Reference 10a. [e] Reference 10b. [f] Reference 31a. [g] Reference 31b. [h] Reference 32. [i] Reference 31c. [j] Reference 24a. [k] Reference 24b.

analogue.[13] Herein, it is possible to evaluate the generality of this correlation. Collected in Table 2 are magnetic data for several complexes with $\{Mn_2O(OAc)_2\}^{2+}$ cores and their Fe analogues.[24−27] In the cases of $[Mn_2O(OAc)_2(HB(pz)_3)_2]$,[13] $[Mn_2O(OAc)_2Cl_2(bpy)_2]$,[10b] $[Mn_2O(OAc)_2(tacn)_2]^{2+}$,[15] and $[Mn_2O(OAc)_2(Me_3tacn)_2]^{2+}$,[15] there is reasonably good agreement between the ratio of the isotropic shifts of the acetate resonances of the manganese and iron complexes and the square of the effective moments, with differences ranging from 5 to 10%. The major exception appears to be the $[Mn_2O(OAc)_2(bpy)_2(H_2O)_2]^{2+}$.[10a] Using the literature values,[10b,24a] the difference in the bpy comparison ranges from 15 to 25%. Indeed, we suggest that the imprecision of the determined $\mu_{eff}^2(Fe)$ value is the source of the variability in the comparison.[24a] Nevertheless, comparisons of the acetate proton resonance isotropic shift ratio ($\Delta H_{Mn}/\Delta H_{Fe}$) to the ratio of the squared effective magnetic moments ($\mu_{eff}^2(Mn)/\mu_{eff}^2(Fe)$) reveal an excellent agreement (within 10%) between these two quantitites.

Additionally, there does appear to be a strong linear correlation between the isotropic shift of the acetate protons and the magnetic coupling contant (J, cm^{-1}) among the various binuclear $Mn_2^{III,III}$ complexes (Figure 4) but not other parameters, such as Mn−O−Mn bond angle. Recently, Satcher and Balch reported a similar correlation for a series of (μ-alkoxo)(μ-X)-dicopper(II) complexes (where X = OAc, NO_2, N_3) over a range of $2J$ from +26 to −1100 cm^{-1}.[28] The isotropic shift of the acetate resonance should serve as a relatively sound guide for estimating the extent of magnetic coupling for new $Mn_2^{III,III}$ binuclear compounds.[7b] Further, the correlation between solid-state magnetic measurements and the solution-state ^1H NMR measurements strongly suggests that the solid-state structure is maintained in solution.

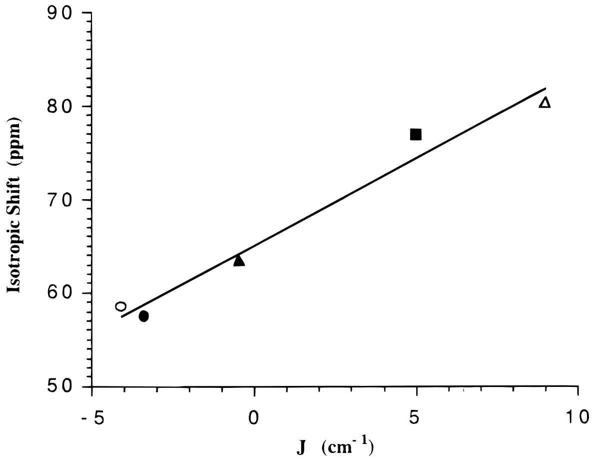

Figure 4. Correlation of the room-temperature chemical shifts of the bridging acetate resonances for a variety of $\{Mn_2O(OAc)_2\}^{2+}$ cores with the magnetic exchange values (J, cm^{-1}). Symbols: ●, **4** (bpy/H_2O); ○, **5** (bpy/Cl); ■, **1** (HB(pz)$_3$); ▲, **2** (tacn); △, **3** (Me_3tacn). The line is a linear regression fit to the points with an R^2 of 0.975.

Acknowledgment. This work was supported by a grant from the National Institutes of Health (GM 38275). We thank Dr. J. G. Boylan for helpful discussions during the preparation of this manuscript.

Supporting Information Available: Synthesis of methyl-substituted ligands, a table of elemental analyses, tables of additional ^1H NMR data showing relative integrated intensisties and T_1 for parent complexes **6**, and figures showing the ^1H NMR spectra for the methyl-substituted complexes examined in this study (8 pages). See any current masthead page for ordering information.

IC960646L